

UAV inspection of large components: indoor navigation relative to structures

Martin Schörner, Michelle Bettendorf, Constantin Wanninger, Alwin Hoffmann, Wolfgang Reif

Angaben zur Veröffentlichung / Publication details:

Schörner, Martin, Michelle Bettendorf, Constantin Wanninger, Alwin Hoffmann, and Wolfgang Reif. 2021. "UAV inspection of large components: indoor navigation relative to structures." In *Proceedings of the 18th International Conference on Informatics in Control, Automation and Robotics - ICINCO, July 6-8, 2021*, edited by Oleg Gusikhin, Henk Nijmeijer, and Kurosh Madani, 179–86. Setúbal: SciTePress.
<https://doi.org/10.5220/0010556301790186>.

UAV Inspection of Large Components: Indoor Navigation Relative to Structures

Martin Schörner^a, Michelle Bettendorf, Constantin Wanninger^b, Alwin Hoffmann^c
and Wolfgang Reif^d

Institute of Software and Systems Engineering, Augsburg University, Universitätsstraße 6a, Augsburg, Germany

Keywords: Inspeciton of Large Components, UAVs, Adaptive Navigation, Sensor Fusion.

Abstract: The inspection of large structures is increasingly carried out with the help of Unmanned Aerial Vehicles (UAVs). When navigating relative to the structure, multiple data sources can be used to determine the position of the UAV. Examples include track data from an installed camera and sensor data from the orientation sensors of the UAV. This paper deals with the fusion of this data and its use for navigation alongside the structure. For the sensor fusion, a concept is developed using a Kalman filter and evaluated simulatively in a prototype. The calculated position data are also fed into a vector flight control system, which dynamically calculates and flies a trajectory along the component using the potential field method. This is done taking into account obstacles detected by the onboard sensors of the UAV. The established concept is then implemented with the Robot Operating System (ROS) and evaluated simulatively.

1 INTRODUCTION

The inspection of large structures using UAVs is becoming increasingly popular. Applications include the inspection of railway tracks (AG,), aircraft (Sappington et al., 2019) or the inspection of ship hulls in dry docks (Englot and S. Hover, 2014). A less common application is the inspection of large components in production. In previous work, we already covered the derivation of a route through inspection points based on a list of part positions (Wanninger et al., 2020). The next step is flying a trajectory that visits all points on the route.

A challenge compared to outdoor flights is, that the usual methods for determining position, such as GPS, work poorly or not at all in a production hall. This requires the use of other sensor data to successfully determine the UAV's position. Since external camera- or radar-based tracking systems are expensive and complex to set up, the work focuses on sensors that can be installed on the UAV. On the one hand, the inertial measurement unit (IMU) of the UAV itself allows for computing a position through odometry.

On the other hand, its inspection camera can be used to orient itself relative to the component. The mapping between the camera image and the real world is not presented in this paper. Problematic parameters such as deviations or latency are simulated. These sensor data are fused in our approach to obtain a more accurate and stable position estimate.


We use this position data to fly the UAV autonomously to inspection points calculated in a previous step. The points are not always approached directly, but a route is calculated with the help of the obstacle detection sensors of the UAV, which avoids unforeseen obstacles along the way. For this purpose, the potential field method (Koren et al., 1991) is used, in which the UAV is attracted to the nearest target point (global minimum) and repelled by detected obstacles (maxima).


The contribution of this paper can be summarized as follows:


- A concept for the fusion of IMU data with camera tracking data to realize an optimal position estimation relative to a component.
- Adaptive navigation of the inspection UAV relative to the inspected part with reaction to obstacles

In the following sections, related work on the subject of inspection by UAVs is presented before the concept for sensor fusion and dynamic navigation is explained

^a  <https://orcid.org/0000-0001-6237-222X>

^b  <https://orcid.org/0000-0001-8982-4740>

^c  <https://orcid.org/0000-0002-5123-3918>

^d  <https://orcid.org/0000-0002-4086-0043>

in more detail. Subsequently, the implementation of the concept is discussed and the results of the evaluation are presented. Finally, a conclusion is drawn and the further procedure is explained.

2 RELATED WORK

For adaptive navigation, different approaches are considered below, which support both orientation to objects and sensor fusions.

In the paper by McAree et al (McAree et al., 2016), a semi-autonomous UAV is used for structural inspections. The UAV is equipped with a laser distance sensor to keep a safe distance from the structure to assist the pilot. For the assistance feature, the robotics framework Robot Operating System (ROS) was used in combination with the simulation environment Gazebo. For the full automatic inspection presented in this paper, ROS is also adopted as the basis.

In (Kawabata et al., 2018) and (Mohta et al., 2018), a depth imaging camera is used instead of a laser sensor, which also provide 3-dimensional mapping of the infrastructure using Simultaneous Localization and Mapping (SLAM). This concept is intended to counteract inaccuracies of the GPS signal in the proximity of infrastructures. However, navigation is based on a two-dimensional mapping of the environment. The solution of T. Zhang et al. (Zhang et al., 2014) also uses SLAM, but in combination with Monte Carlo simulation. Navigation also takes place in 2-dimensional space with a laser sensor. The sonar sensor is only used for the detection of glass.

In the work of L. V. Santana et al. (Santana et al., 2014), multiple sensors are fused by a simple Kalman filter for position tracking. The odometric data of the UAV and an ultrasonic sensor are used. On the opposite side, the advantages of an extended Kalman filter for nonlinear acceleration in the field of UAVs is presented by Belokon et al. (Zolotukhin et al., 2013). In this project, a trajectory with an average deviation of 0.2m could be flown indoors with only one camera in combination with UAV odometry. In contrast, a similar project by Shen et al. (Shen et al., 2013) achieves an average deviation of 0.5 m with stereoscopic cameras, but at a speed of 4 m/s.

This paper combines the sensor fusion of a simulated tracking camera with the odometry of a copter and complements it with an adaptive collision detection and avoidance strategy in an indoor szenario.

3 CONCEPT

In our use case, we assume that a larger structure in a production hall is to be inspected by a UAV. For this purpose, the UAV must fly to a sequence of inspection points from which it can examine relevant parts of the structure (Wanninger. et al., 2020). In the following, we first give an overview of the overall concept for flying this sequence of points. Then the individual components of the architecture are explained in more detail. These include the determination of the position without external sensors and the navigation to the respective inspection points while avoiding collisions with obstacles.

3.1 Architecture Overview

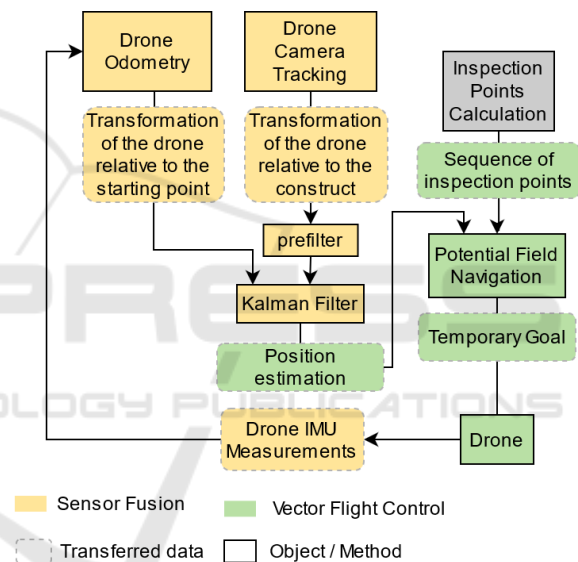


Figure 1: Sensor data of the camera tracking and the drone odometry are fed to the Kalman filter which uses these values to estimates a new position. The estimated position is used for the potential filed navigation.

The overall architecture of the system can be split into two interconnected parts (see Fig. 1), the sensor fusion (green) and the navigation system (yellow). The IMU provides the estimated position of the UAV relative to the starting point. Additionally the inspection camera can be used to get position information relative to the inspected structure through optical tracking algorithms (see (Shen et al., 2013), (Mohta et al., 2018)). Data from the two input sources can be used as input for the Kalman filter (Wan and Van Der Merwe, 2000), which in turn outputs a more accurate position estimation. In this paper, a normal Kalman filter is used instead of an EKF or UKF (Wan and Van Der Merwe, 2000) because after lineariza-

tion, the accuracy of the linearized system is sufficient for our use case as shown in the evaluation. The position estimation is used as measured process variable for the vector flight control. The flight control iterates over a set of inspection points and generates temporary setpoints to navigate through the potential field towards the next point. The UAV then feeds back its IMU data to the Kalman filter and new camera tracking data is continuously generated to complete the control loop.

3.2 Sensor Fusion of UAV Odometry and Camera Tracking Data

The aim of sensor fusion is to combine different sensor and tracking data to produce a more accurate position estimate. The position should not be determined in a global coordinate system, but in relation to the component. For this purpose, the IMU data of the UAV as well as the position determined by camera tracking are used in our example. The odometry data provides the transformation from the starting point of the UAV to its current location and has a relatively steady course without jumps. However, the determined position drifts from the actual value over time due to the dual integration of the IMU's accelerometer data. Camera tracking of the camera installed on the UAV determines the position of the UAV relative to the viewed component. A drift does not occur with visual tracking. However, under poor visibility conditions, the tracking can briefly output incorrect positions and thus lead to jumps in the position data. To combine the advantages of both sensors and to mitigate their disadvantages as far as possible, we use a Kalman filter to combine the two measured transformations. Due to the fact that the acceleration of the UAV is non-linear, the system has to be linearized in order to be used in conjunction with a standard Kalman filter. For the linearization, the mean velocity for each axis direction (x, y, z) as well as the rotational velocity around the yaw axis will be calculated in every step. As shown below using the velocity of the x-axis as an example, the velocities are calculated by dividing the change in position from time t to $(t + T)$ by the time difference since the last update (T).

$$v_x = \frac{x(t+T) - x(t)}{T} \quad (1)$$

The linearization of y, z and yaw is performed analogously. The estimated position from the Kalman filter is then used for the trajectory planning.

3.3 Vector Flight Control

In this project, a feasible path which is as short as possible and collision-free has to be computed out of a sequence of given view points. The planning will be done online due to the fact, that in later iterations, the UAV should be able to avoid dynamic obstacles that occur at runtime. Because of these constraint a vector flight control based on a computed artificial potential field (Chen et al., 2016) was used. The controller generates a potential field based on the current goal and obstacles in the world. The goal represents a strong, attracting force, whereas any obstacles have repulsive potentials around them. The general idea is that at any given point in the potential field the goal position can be reached by following the potential vector at the UAV's current position. Static obstacle positions are either derived from the CAD-File of the assembly or defined manually. Figure 2 shows an example of a UAV navigating to a goal point around a static obstacle. In this example, the attracting potential of the

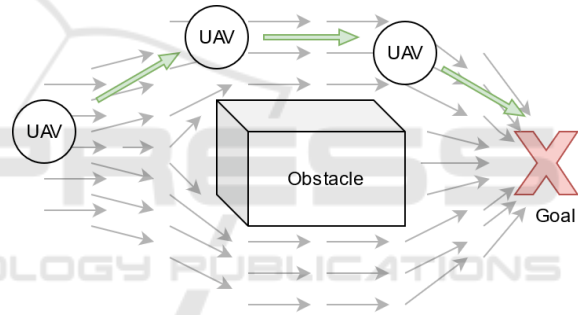


Figure 2: UAV navigating around an obstacle in a potential field.

goal pulls the UAV to the left. The obstacle between the UAV and the goal alter the potential field in a way that causes the UAV to fly around it. This method works great with obstacles that are known in advance (e.g. the inspected structure and its fixtures, walls...)

In order to react to dynamic obstacles like people or tool carts, an extension of this strategy is needed. Many UAV have onboard collision avoidance sensors that can detect obstacles in the surroundings of the UAV. In order fly around these obstacles, the collision avoidance data can be used to dynamically add obstacles to the potential field and recalculate the potentials based on the new obstacles. By doing this, the UAV avoids previously known and unforeseen obstacles.

One drawback of the potential field method is that local minimum traps can appear. The goal should always be the global minimum. However, local minima can occur and if the UAV gets pulled into one of these minima by the potential, it gets stuck there.

For solving this issue, we first detect, if the UAV is stuck in a local minimum by checking if its position stays within a small area for longer periods of time. We then generate a random point in space as a new, temporary goal and adjust the potential field to accommodate the new goal. The random walk method is illustrated in figure 3. The robot is moving in a random direction, which does not collide with the obstacle. The UAV then approaches the temporary goal for a certain amount of time to get out of the local minimum (see step 2 of Fig. 3). After some time, actual destination point is set as the goal again and the UAV either continues towards it or flies back to the local minimum. If the UAV flies back to the local minimum, the procedure is repeated until the minimum is escaped.

If the UAV reaches the same minimum for multiple times, there is a possibility that there is no way to get out of the local minimum. In this case an abort scenario can be defined where the UAV returns to its original starting point and lands after a certain number of unsuccessful escape attempts.

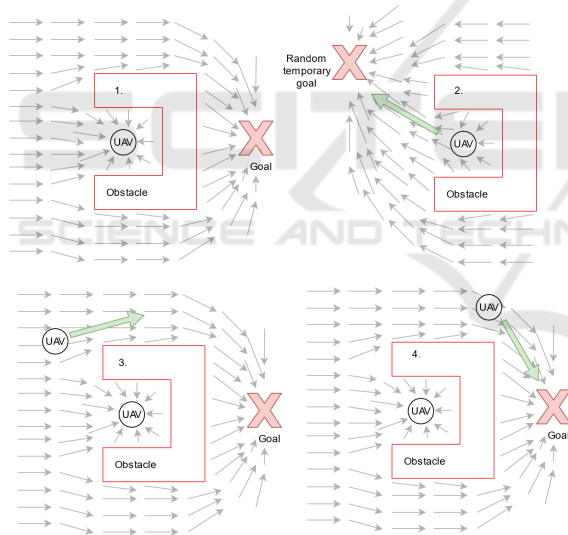


Figure 3: Escaping the local minimum by defining a random temporary goal.

With these strategies the UAV is able to safely fly to an inspection point without colliding with its surroundings. Completing a whole inspection is simply a matter of flying to each of the inspection points of the given sequence using the method described in this subsection.

4 IMPLEMENTATION

The following section describes the implementation of the concept described in 3. It was implemented using the robotic framework Robot Operating System (ROS). For the simulation of the UAV we used RotorS (Furrer et al., 2016).

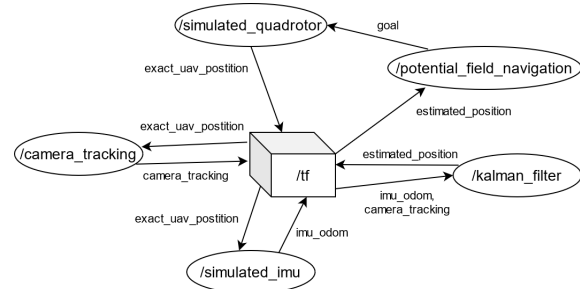


Figure 4: Communication of the implemented ROS nodes. The camera tracking and imu odometry calculate their simulated sensor values based of the exact drone position. The Kalman filter node uses these positions to create an estimate which is in turn used by the potential field navigation to control the simulated quadrotor.

4.1 Simulated Sensors

In a first step, the concept was implemented within a simulation. Therefore, sensors with similar properties to their real counterparts were implemented. The simulated camera tracking data calculates the exact transformation from the UAV to the part to be inspected and adds “jumps” to the position at randomized times to simulate tracking errors. This is done by generating uniformly distributed random distances between 2 and 4 m and adding them to the translation. The UAV’s odometry is generated by calculating the transformation from the UAV’s starting point to its current position. After that an offset that is increasing by 0.00001 m each step is added to each axis of the transformation to simulate an error due to drift.

4.2 Kalman Filter

The simulated sensor values are used by the Kalman filter to generate a position estimation. Figure 4 shows the Kalman filter receiving the simulated IMU and camera tracking sensor data. The camera position is passed through a pre-filter that eliminates big jumps in the camera tracking (see Fig. 1). Since acceleration of the UAV is finite, it can only move a certain amount in one control loop. If the change in the position of the UAV exceeds a predefined threshold, the measurement is discarded. After this prefilter step,

both sensor inputs are passed to the actual Kalman filter. The actual Kalman filter was implemented using the filterpy python library (Labbe, 2021).

The state matrix X contains the system states. It is defined as: $[x, vx, y, vy, z, vz, yaw, vyaw]^T$. The velocities are calculated by the numerical differentiation of the position. The state transition matrix F is used to generate the state for the next timestep.

$$F = \begin{pmatrix} 1 & dt & 0 & 0 & 0 & 0 & 0 & 0 \\ 0 & 1 & 0 & 0 & 0 & 0 & 0 & 0 \\ 0 & 0 & 1 & dt & 0 & 0 & 0 & 0 \\ 0 & 0 & 0 & 1 & 0 & 0 & 0 & 0 \\ 0 & 0 & 0 & 0 & 1 & dt & 0 & 0 \\ 0 & 0 & 0 & 0 & 0 & 1 & 0 & 0 \\ 0 & 0 & 0 & 0 & 0 & 0 & 1 & dt \\ 0 & 0 & 0 & 0 & 0 & 0 & 0 & 1 \end{pmatrix} \quad (2)$$

The measurement matrix H is used to connect the measurements to the states and was defined as a identity matrix (I). The control transition matrix B is defined as $[0,0,0,0]^T$. For measurement and process noise R and Q , the value $0.2 \cdot I$ was determined empirically. The system state variable is initialized with the initial position of the odometry and a velocity of zero. In each step, a prediction is made using the system model of the Kalman filter. Afterwards, new sensor values of the odometry and the cameratracking are derived from the ROS TF graph. These values are then used to correct the state estimation of the Kalman filter. As a last action, the calculated estimated position of the Filter is published to the TF graph. This position is then used by the navigation stack to reach the predefined inspection points.

4.3 Potential Field Method Implementation

The inspection points (route) are generated in a previous step, presented in (Wanninger, et al., 2020) and loaded by the navigation node which tries to reach these points sequentially. For reaching each inspection point the potential field method is used, a vector based navigation with attracting (targets) and repelling (obstacles) potentials. Instead of taking the inspection point as the target point, our approach creates temporary intermediate targets in each iteration that are approached by the UAV but never reached. This procedure is necessary because due to proprietary interfaces of the UAV only points and no direction vectors can be submitted. The targets (x) are regularly recalculated based on the current potential acting on the UAV, so that potentially dynamic obstacles can also be taken into account.

$$x = x + r * fx \quad (3)$$

The force in x-direction (fx) is internally defined cyclically, while the rate (r) is a constant that globally defines the distance of the new targets from the current UAV position and was set to 0.5 in our tests. The equations for the y and z position are performed analogously. The resulting temporary target is redefined in fixed time cycles until an inspection point is reached which can be defined with a deviation, in our tests this is set to 30cm.

To prevent the UAV from getting stuck in a local minimum, e.g. a U-shaped obstacle, the random walk method is utilized. If the UAV has not moved significantly within the last time cycle, it is assumed that the UAV has encountered a local minimum. To get out of the local minima, new targets are randomly created each time cycle for the UAV to reach, taking into account potential repulsive forces. This is repeated until a target is found that leads out of the minima. After leaving the local minima, the distance to the viewpoint is recalculated and the last position is updated to avoid an infinite loop. If no solution to the local minima is found after a defined time, manual intervention is required. When an inspection point is reached, the process is repeated with the next inspection point of the route. In a real scenario, the actual inspection must be performed before proceeding to the next inspection point.

5 EVALUATION

The evaluation is structured in three parts. Initially the sensor fusion was evaluated by introducing errors into the camera tracking and imu position. As a second step, the vector flight control was tested with using the exact UAV position. Finally, the position estimated by the Kalman filter was used to navigate to a sequence of viewpoints using the vector flight control.

5.1 Sensor Fusion Evaluation

The evaluation of the Kalman filter is done by manually flying the UAV to predefined points. During flight, the exact position of the UAV is recorded and compared to the output of the Kalman filter. For simplicity we only show one axis of the UAV's movement. Each graph contains the simulated odometry of the UAV (blue), the simulated tracking data (green) and the output of the Kalman filter (red). The positions are calculated in relation to the starting position of the UAV.

Initially a control flight is performed, where both sensors report the exact UAV position without any errors. Figure 5 shows how the output of the Kalman

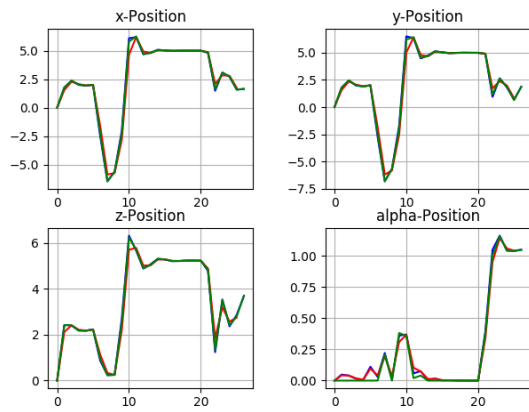


Figure 5: Output of the Kalman filter (red) with drift-free imu-position (blue) and jump-free camera tracking data (green).

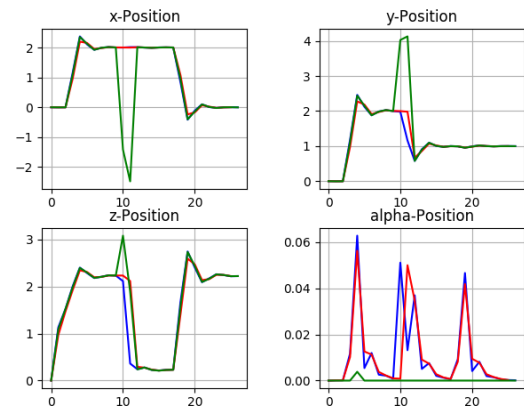


Figure 7: Output of the Kalman filter (red) with drift-free imu-position (blue) and jumps in the camera tracking (green).

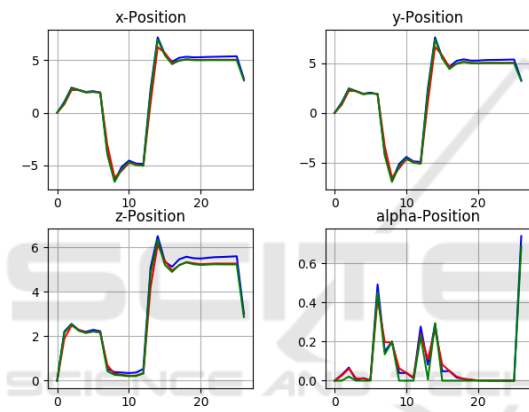


Figure 6: Output of the Kalman filter (red) with drifting imu-position (blue) and jump-free camera tracking data (green).

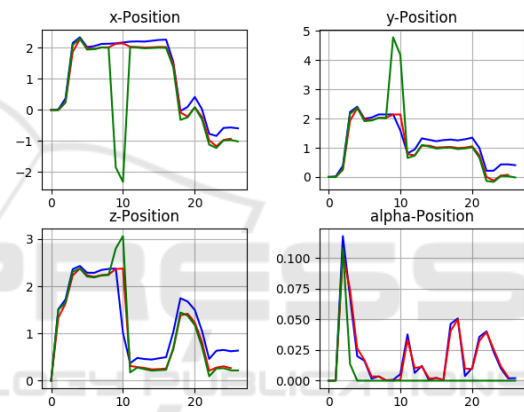


Figure 8: Output of the Kalman Filter (red) with drifting imu-position (blue) and jumps in the camera tracking (green).

filter follows the sensor data input.

In the next step, we introduced a slowly increasing drift into the IMU position. Figure 6 shows how the drift only minimally influences the output of the Kalman filter.

We also tested the influence of jumps in the camera tracking along with clean IMU data (7). Since the prefilter keeps these jumps from getting to the Kalman filter, the output remains unaffected of the jump.

Finally, we fed the Kalman filter the drifting IMU data and introduced jumps in the camera tracking data (see Fig. 8). With increasing drift of the IMU position, the Kalman filter trusts the camera tracking data. When the tracking data cuts out due to the jump, the estimate deviates towards the drifting IMU position, but recovers as soon as the tracking data is available again.

The evaluation of the Kalman filter shows, that errors like an increasing drift or jumps only influence

the position estimate minimally. Therefore the estimated position can be used for the evaluation of the vector flight control.

5.2 Vector Flight Control Evaluation

The goal of the vector flight controller is to reach all inspection points while avoiding static obstacles. For evaluating the vector flight control, the position estimation from the Kalman filter is neglected at first and the exact position values are used instead.

In the evaluation scenario the UAV needs to reach a sequence of three points in 3-dimensional space.

Viewpoint	x	y	z	yaw
1	4m	1m	1m	1 degree
2	6m	-1m	2m	2 degree
3	2m	-2m	3m	1 degree

The point is considered as reached, if the position of the UAV deviates less than 0.3m from the point.

One problem that can occur during navigation is the UAV getting stuck in a local minimum of the potential field. The obstacle that causes the minimum in the potential field is shaped like the letter “U” (see Fig. 3). Figure 9 shows the reaction to a u-shaped local minimum trap when only using the potential field method. The UAV is trapped around $(2.5, -0.25, 2.5)$, because of the u-shaped obstacle. The goal is set to $(5, -3, 10)$. The UAV can't escape the trap using the potential field method alone. This is why in the next pass, the random walk method mentioned in the concept was is performed to escape the minimum. Figure 10 shows the movement of the UAV with the same goal as in figure 9, but with the implemented random walk method. The random walk method caused the UAV to fly out of the local minimum, which can be mainly seen in the x position in figure 10. It took the random walk strategy three tries to escape the local minimum completely. After that, the potential field method was used again to reach the actual goal without colliding with any obstacles.

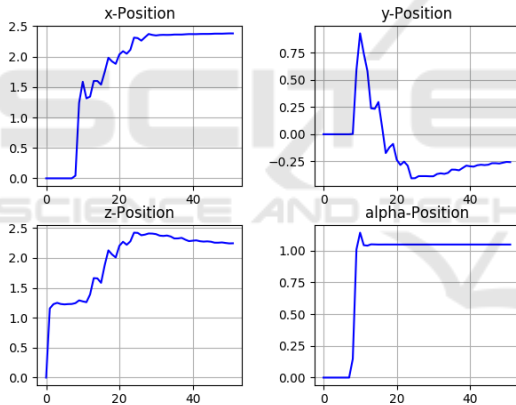


Figure 9: UAV stuck in a local minimum at $(2.5, -0.25, 2.5)$.

5.3 Evaluation of the Combined Architecture

After evaluating the sensor fusion and the navigation separately, a final test was used to evaluate the combination of the two procedures. The UAV was given multiple goals to fly to sequentially while using the position estimation generated by the Kalman filter. The filter was fed with a drifting IMU position and tracking data that had jumps in it. Figure 11 shows that the filtered position (red) is just slightly affected by the drift in the odometry data (blue) or the jump in the camera tracking (green). Despite the two poor input signals, the UAV manages to reach all targets within the specified precision of 0.3m .

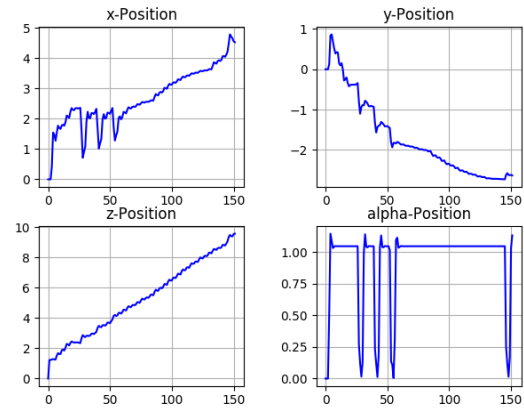


Figure 10: UAV using the random walk method to escape the local minimum at $(2.5, -0.25, 2.5)$ by flying towards a random temporary goal before continuing to the actual goal at $(5, -3, 10)$.

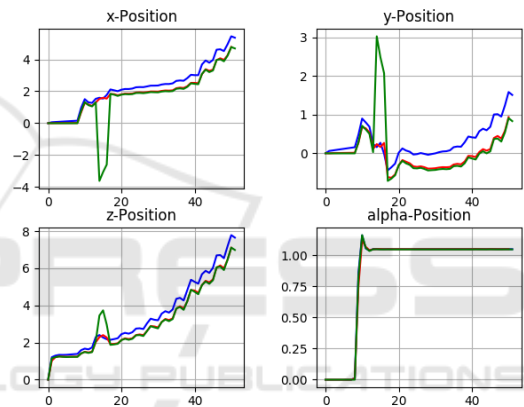


Figure 11: UAV flying to multiple viewpoints while getting its position from faulty sensor data.

The evaluation has shown that the output of the Kalman filter in combination with a prefilter for the cameratracking improves the quality of the position data compared to the use of a single sensor as a position source. Our flight control algorithm is capable of reaching a sequence of waypoints while avoiding static obstacles, even when using the position estimation provided by the Kalman filter. It was also demonstrated, that the algorithm can handle being stuck in a local minimum of the potential field.

6 CONCLUSIONS

This paper covered the inspection of a large structure like a ship hull. The addressed topics are sensor fusion and vector flight control. To estimate the position of the UAV the internal IMU and tracking from the inspection camera were used. These signals with differ-

ent fault characteristics were fused by a Kalman filter. The camera tracking signal was pre-filtered before it was sent to the Kalman filter in order to filter out harsh jumps in the tracked position. The estimated position was fed to a vector flight control based on the potential field method, which allowed the UAV to reach a sequence of inspection points without colliding with obstacles in its environment. We also proposed a solution for the local minimum problem using the random walk. In our evaluation we demonstrated that fusing the two sensor values creates an estimate, that is robust to faulty inputs of one of the sensors. Additionally we demonstrated, that our navigation concept allows the UAV to reach a sequence of inspection points while avoiding surrounding obstacles. Finally it was shown that the navigation works in conjunction with the position estimate calculated by the Kalman filter. In the future, we are planning on implementing the proposed algorithms on real hardware. Additionally, we plan on expanding the navigation to react to dynamic obstacles that are not known in advance. This can be done by dynamically placing obstacles that are detected by the UAV in the potential field and recalculating the force vector based on the new data. Finally, using a sensor that tracks the position of the UAV relative to the part and not relative to a global coordinate system, could allow the UAV to navigate relative to the part even when it is in motion. This would allow inspections of a structure while it is being craned from one assembly station to another one. The feasibility of this concept will have to be evaluated in future work.

ACKNOWLEDGEMENTS

This work was created in collaboration with Kevin Dittel, Teoman Ismail, Christian Adorian and Åsa Odenram from Premium AEROTEC GmbH.

REFERENCES

- AG, D. B. Kompetenzcenter multicopter db. last accessed: 08.03.2021.
- Chen, Y.-b., Luo, G.-c., Mei, Y.-s., et al. (2016). Uav path planning using artificial potential field method updated by optimal control theory. *International Journal of Systems Science*, 47(6):1407–1420.
- Englot, B. and S. Hover, F. (2014). Sampling-based coverage path planning for inspection of complex structures. *ICAPS 2012 - Proceedings of the 22nd International Conference on Automated Planning and Scheduling*.
- Furrer, F., Burri, M., Achtelik, M., and Siegwart, R. (2016). Rotors—a modular gazebo mav simulator framework. In *Robot operating system (ROS)*, pages 595–625. Springer.
- Kawabata, S., Nohara, K., Lee, J. H., et al. (2018). Autonomous flight drone with depth camera for inspection task of infra structure. In *Proceedings of the International MultiConference of Engineers and Computer Scientists*, volume 2.
- Koren, Y., Borenstein, J., et al. (1991). Potential field methods and their inherent limitations for mobile robot navigation. In *ICRA*, volume 2, pages 1398–1404.
- Labbe, R. R. (2021). Filterpy documentation. last accessed: 08.03.2021.
- McAree, O., Aitken, J. M., and Veres, S. M. (2016). A model based design framework for safety verification of a semi-autonomous inspection drone. In *2016 UKACC 11th International conference on control (CONTROL)*, pages 1–6. IEEE.
- Mohta, K., Sun, K., Liu, S., et al. (2018). Experiments in fast, autonomous, gps-denied quadrotor flight. In *2018 IEEE International Conference on Robotics and Automation (ICRA)*, pages 7832–7839. IEEE.
- Santana, L. V., Brandao, A. S., Sarcinelli-Filho, M., and Carelli, R. (2014). A trajectory tracking and 3d positioning controller for the ar. drone quadrotor. In *2014 international conference on unmanned aircraft systems (ICUAS)*, pages 756–767. IEEE.
- Sappington, R. N., Acosta, G. A., Hassanalian, M., et al. (2019). Drone stations in airports for runway and airplane inspection using image processing techniques. In *AIAA Aviation 2019 Forum*, page 3316.
- Shen, S., Mulgaonkar, Y., Michael, N., and Kumar, V. (2013). Vision-based state estimation and trajectory control towards high-speed flight with a quadrotor. In *Robotics: Science and Systems*, volume 1, page 32. Citeseer.
- Wan, E. A. and Van Der Merwe, R. (2000). The unscented kalman filter for nonlinear estimation. In *Proceedings of the IEEE 2000 Adaptive Systems for Signal Processing, Communications, and Control Symposium (Cat. No. 00EX373)*, pages 153–158. Ieee.
- Wanninger, C., Katschinsky, R., Hoffmann, A., Schörner, M., and Reif, W. (2020). Towards fully automated inspection of large components with uavs: Offline path planning. In *Proceedings of the 17th International Conference on Informatics in Control, Automation and Robotics - Volume 1: ICINCO*, pages 71–80. INSTICC, SciTePress.
- Zhang, T., Chong, Z. J., Qin, B., et al. (2014). Sensor fusion for localization, mapping and navigation in an indoor environment. In *2014 International Conference on Humanoid, Nanotechnology, Information Technology, Communication and Control, Environment and Management (HNICEM)*, pages 1–6.
- Zolotukhin, Y. N., Kotov, K. Y., Mal'tsev, A., et al. (2013). Using the kalman filter in the quadrotor vehicle trajectory tracking system. *Optoelectronics, Instrumentation and Data Processing*, 49(6):536–545.